Azbel'-Kaner Cyclotron Resonance in Thallium*

JERRY C. SHAW† AND GLEN E. EVERETT
Department of Physics, University of California, Riverside, California 92502
(Received 2 June 1969)

The angular dependence of Azbel'-Kaner cyclotron resonance in single crystals of high-purity thallium has been investigated at 24 GHz and 1.4°K for sample surfaces perpendicular to the three principal crystallographic directions. These measurements have revealed sections of Fermi surface not previously reported. Detailed comparisons are made with the nearly free-electron Fermi surface and with Soven's relativistic orthogonalized-plane-wave calculations. While several orbits were observed to be compatible with these models, other orbits were observed which we are unable to assign using either model. Cyclotron resonance for magnetic field directions making oblique angles with a $(10\bar{1}0)$ surface has also been investigated. These studies revealed highly anisotropic, large-amplitude resonances for magnetic field directions making angles of up to 80° with the sample surface. These resonances have been attributed to extended orbits that are possible because of magnetic breakdown effects. The extended-orbit mechanism proposed by Khaikin and Cheremisin was found to account qualitatively for the observed behavior. The experimentally determined masses were quantitatively compared with the nearly free-electron predictions, resulting in estimates of the mass enhancement factors ranging from 1.4 to 1.8. These values were found to disagree with the most recent determinations of the specification-heat mass enhancement factor.

I. INTRODUCTION

FOR several years, the only available model of the Fermi surface (FS) of thallium was Harrison's[1] nearly free-electron (NFE) model. Studies of the magnetoacoustic effect by Rayne[2] and of the magnetoresistance by Alekseevski and Gaidukov[3] and by Makintosh *et al.*[4] confirmed its qualitative validity. More recently, a relativistic, orthogonalized-plane-wave (ROPW), electronic band-structure calculation was performed by Soven.[5] The FS resulting from these calculations is qualitatively similar to the NFE model using the single-zone scheme; however, important differences exist, mainly with respect to connectivity in the [0001] direction.

Several workers have observed good agreement with the predictions of the ROPW model for the larger surfaces of the third and fourth zones, and, in addition, have observed considerable evidence of magnetic breakdown effects. Priestley[6] conducted pulsed-field de Haas–van Alphen studies and concluded that the observed areas attributed to the large third-zone hole surface and the fourth-zone electron surface were in good agreement with the ROPW model. However, no detailed information was given for the smaller sections of the FS. Similar conclusions concerning the third- and fourth-zone surfaces of the ROPW model were drawn by Eckstein *et al.*[7] and by Coon *et al.*,[8] from the results of their magnetoacoustic measurements. In addition, the later group reported some detailed information concerning the smaller sections of the FS. Recent magnetoresistance studies have been conducted by Milliken and Young,[9] while detailed studies of magnetic breakdown effects as observed in the magnetoresistance have been made by Young.[10] With the exception of the results of Rayne, all of the above studies indicate that the FS of thallium is not connected in the [0001] direction, in agreement with the ROPW model.

A recent study of the Azbel'-Kaner cyclotron resonance effect was conducted by Dahlquist and Goodrich[11] (DG). Our study has revealed resonances that are due to sections of the FS that have not previously been reported. In addition, certain discrepancies appear to exist between our results and those of DG. Part of the following discussion is devoted to the presentation of assignments, alternative to those of DG, that arise as a result of these discrepancies.

Section II briefly reviews the theoretical aspects of cyclotron resonance, while Sec. III describes the experimental procedures. In Sec. IV, a description of both the NFE and ROPW FS models is given. Section V is devoted to a detailed analysis and discussion of results, and finally, a summary and concluding remarks are given in Sec. VI.

II. THEORY OF AZBEL'-KANER CYCLOTRON RESONANCE

Azbel'-Kaner cyclotron resonance has been observed in many metals since the original paper[12] predicting this effect. As a result of their work, an entire field concerning the interaction of electromagnetic radiation with metals has developed. An excellent review, in-

* This work was supported by the National Science Foundation.
† Present address: Solid State Science Division, Argonne National Laboratory, Argonne, Ill. 60439.
[1] W. A. Harrison, Phys. Rev. **118**, 1190 (1960).
[2] J. A. Rayne, Phys. Rev. **131**, 653 (1963).
[3] N. E. Alekseevskii and Y. P. Gaidukov, Zh. Eksperim. i Teor. Fiz. **43**, 2094 (1962) [English transl.: Soviet Phys.—JETP **16**, 1481 (1963)].
[4] A. R. Mackintosh, L. E. Spanel, and R. C. Young, Phys. Rev. Letters **10**, 434 (1963).
[5] P. Soven, Phys. Rev. **137**, A1706 (1965); **137**, A1717 (1965).
[6] M. G. Priestley, Phys. Rev. **148**, 580 (1966).
[7] Y. Eckstein, J. B. Ketterson, and M. G. Priestley, Phys. Rev. **148**, 586 (1966).
[8] J. B. Coon, C. G. Grenier, and J. M. Reynolds, J. Phys. Chem. Solids **28**, 301 (1967).
[9] J. C. Milliken and R. C. Young, Phys. Rev. **148**, 558 (1966).
[10] R. C. Young, Phys. Rev. **163**, 676 (1967).
[11] W. L. Dahlquist and R. G. Goodrich, Phys. Rev. **164**, 944 (1967).
[12] M. Ia. Azbel' and E. A. Kaner, Zh. Eksperim. i Teor. Fiz. **32**, 896 (1956) [English transl.: Soviet Phys.—JETP **5**, 730 (1957)].

cluding cyclotron-resonance effects, has been given in a two-part series by Mertsching.[13] In addition, Kip and co-workers[14–16] have conducted detailed experimental studies of cyclotron resonance as a tool for determining features of the FS, while further studies have been conducted by Shaw *et al.*[17,18]

Under the conditions for observation of the anomolous skin effect,[19] the microwave electric field strength is no longer an exponentially decaying function of the depth into the metal but goes to zero rather abruptly at some finite depth of the order of the classical skin depth δ. If, in addition, carriers in a metal, subjected to a magnetic field parallel to a planar surface, execute cyclotron trajectories with radii $r \gg \delta$ and with cyclotron periods $T_c \ll \tau$, where τ is the mean free time between collisions, then they can interact repeatedly with the microwave electric field in the skin depth. At resonance, when the cyclotron period is an integral multiple of the microwave period, these carriers can resonantly absorb energy from the incident radiation, giving rise to an increase in the microwave conductivity with a resultant decrease in the surface impedance. This relation between the microwave frequency and the applied field for resonance is given by

$$1/H_n = ne/\omega_{\mathrm{mw}} m^* c\,, \tag{1}$$

where n is an integer, e is the electronic charge, ω_{mw} is the angular frequency of the microwave field, m^* is the cyclotron mass, and c is the speed of light. Azbel' and Lifshitz[20] have shown that when the microwave period is considerably less than τ, the resonant field values of Eq. (1) can be determined with reasonable accuracy from the positive peaks in the field derivative of the real part of the surface impedance, dR/dH. Thus, plots of the inverse-field values of these peaks in dR/dH versus integers yields a straight line, the slope of which is proportional to the inverse of m^*.

The cyclotron mass is related to features of the FS by the expression[21]

$$m^*(k_H) = \frac{\hbar^2}{2\pi} \frac{\partial S(k_H,E)}{\partial E}\bigg|_{E=E_F}, \tag{2}$$

where E_F is the Fermi energy and $S(k_H,E)$ is the cross-section area in k space defined by the intersection of a constant-energy surface and the plane normal to **H** given by $k_H = \mathbf{k}\cdot\mathbf{H}/|H| =$ a constant. In general, observed resonances are due to orbits arising from sections of FS for which m^* is extremal or nearly so with respect to variations in k_H, i.e., $\partial m^*/\partial k_H \approx 0$.[22] The anisotropy of these extremal masses is determined experimentally and detailed comparisons are subsequently made with existing FS models.

Harrison[23] has shown that the orbit-average velocity component along **H** is given by

$$\langle v_H \rangle = \frac{-\hbar}{2\pi m^*} \frac{\partial S(k_H,E_F)}{\partial k_H}. \tag{3}$$

For field directions tipped slightly out of the plane of the sample surface, those electrons with $\langle v_H \rangle \neq 0$ may drift out of the skin depth before completing τ/T_c revolutions. In this case, the amplitude of the resonances will diminish as the angle of tipping is increased. For orbit planes that include a center of inversion, $\partial S/\partial k_H = 0$ for any orientation of **H** and the strengths of the resonances from these orbits will be relatively unaffected by field tipping. Thus, by tipping the field out of the surface of the sample, added information may be gained concerning the origin of carriers contributing to observed resonances. In addition, Koch *et al.*[15] have shown that measurements made with the magnetic field tipped out of the plane of the sample may produce erroneous values for m^*. This effect is characterized by nonzero integer-axis intercepts (phase shifts) in the plot of the $1/H$ values of the dR/dH peaks versus integers. This characteristic may be utilized to determine when the field is parallel to the sample surface, as well as to give a measure of the surface flatness.

III. EXPERIMENTAL PROCEDURE

Zone-refined bars of thallium with a quoted impurity content of less than 1 part per million (including sulphur) were purchased from Cominco Products Inc. Various methods were used for growing single-crystal samples suitable for these measurements. A modified strain-anneal technique, similar to that used by Saunders and Lawson,[24] was used to grow several large crystals. Resistance ratios ($\rho_{300°}/\rho_{4.2°}$) of 8600 were measured for these samples. A very large monocrystal (450 g) was obtained by vacuum (10^{-6} Torr) drip-melting the metal into a graphite crucible and subsequently reducing the temperature through the bcc-hcp phase transition at 503° K[25] over a several-day period. The drip-melter and crucible were machined from high-

[13] J. Mertsching, Phys. Status Solidi **14**, 3 (1966); **26**, 9 (1968).
[14] A. F. Kip, D. N. Langenberg, and T. W. Moore, Phys. Rev. **124**, 359 (1961).
[15] J. F. Koch, R. A. Stradling, and A. F. Kip, Phys. Rev. **133**, A240 (1964).
[16] F. W. Spong and A. F. Kip, Phys. Rev. **137**, A431 (1965).
[17] M. P. Shaw, P. I. Sampath, and T. G. Eck, Phys. Rev. **142**, 399 (1966).
[18] M. P. Shaw, T. G. Eck, and D. A. Zych, Phys. Rev. **142**, 406 (1966).
[19] G. E. H. Reuter and E. H. Sondheimer, Proc. Roy. Soc. (London) **A195**, 336 (1948).
[20] M. Ia. Azbel' and I. M. Lifshitz, in *Progress in Low Temperature Physics*, edited by C. J. Gorter (North-Holland Publishing Co., Amsterdam, 1961), Vol. 3, p. 288.
[21] See any solid-state text, e.g., C. Kittel, *Quantum Theory of Solids* (John Wiley & Sons, Inc., New York, 1963).
[22] This is in contrast to the de Haas–van Alphen effect, which measures extremal areas. These two methods measure properties of the same k-space orbit when the plane of the orbit includes a center of inversion, i.e., central orbits.
[23] Reference 1, p. 1202.
[24] G. A. Saunders and A. W. Lawson, Phys. Rev. **135**, A1161 (1964).
[25] *Metals Reference Book*, edited by C. J. Smithels (Butterworth's Scientific Publications, Ltd., London, 1962).

purity graphite,[26] and before use were outgassed for several hours in a 10^{-6} Torr vacuum at 1700°C.

A Servomet spark-erosion machine was initially used to cut samples. A reasonable degree of success was attained for sample surfaces lying in the (0001) plane; however, the sample surfaces lying in $(11\bar{2}0)$ and $(10\bar{1}0)$ planes exhibited considerable spark-erosion damage even when cut with the lowest spark-energy setting. The large single crystal obtained from the vacuum-melting process was cut using an Agietron[27] spark-erosion machine. A cutting tool consisting of a moving 0.4-mm-diam copper wire was used. During cutting, a very sensitive servo system prevented the moving wire from touching the sample while maintaining 45 V between them. In spite of these precautions, visible damage was observed for the $(11\bar{2}0)$ sample. Shearing on the close-packed planes of the crystal in the $[11\bar{2}0]$ direction was visually observed. Cutting the $(10\bar{1}0)$ surface on the same single crystal using the same technique did not produce visible damage. The two resulting disks (6.3 mm thick by 32 mm diam) were etched by dipping into a solution of 4 parts glacial acetic acid and 1 part 30% hydrogen peroxide. A considerable amount of metal was taken off by this method, leaving the $(11\bar{2}0)$ and $(10\bar{1}0)$ samples in the shape of disks 3 mm thick by 25 mm diam. The surfaces of these samples were still reasonably planar and were ready for polishing. The $(11\bar{2}0)$ sample was annealed for several days at approximately 495°K, while the $(10\bar{1}0)$ sample received no subsequent anneal. These were the best samples obtained for these planes and data from both are reported. The data from the $(10\bar{1}0)$ sample surface exhibited values of $\omega_{mw}\tau$ greater than 65 for some resonances, while the data from the $(11\bar{2}0)$ sample, with comparable surface quality, exhibited considerably lower values of $\omega_{mw}\tau$. Although certainly not conclusive, these observations support the contention that the spark-erosion process produces damage at considerable depths into the bulk of thallium, particularly in the $[11\bar{2}0]$ direction. Spark-erosion damage in single crystals of niobium has been reported in a study by Guberman.[28] The fact that all previous thallium FS studies have been conducted on samples cut and planed by the spark-erosion process may account for the lack of evidence of certain sections of the FS that have been observed in the present study.

Sample surfaces were polished by allowing the samples to glide across the cloth-covered surface of a glass slide immersed in a polishing solution. A polishing solution consisting of the same acetic-acid–hydrogen-peroxide mixture described above was used for the (0001) surface, while concentrated nitric acid was used for the $(10\bar{1}0)$ and $(11\bar{2}0)$ surfaces. These surfaces were oriented to within ±1° by use of Laue back-reflection photographs. Because of thallium's rapid oxidation in air, it was necessary that samples be immediately immersed in anhydrous glycerine upon termination of the polishing phase.

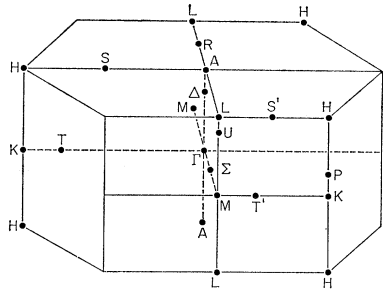

FIG. 1. Brillouin zone for the hexagonal lattice.

The polished sample surfaces formed the end wall of a rectangular cavity operated in the TE_{101} mode at a frequency of 24 GHz. The cavity was equipped with a gear mechanism designed to rotate the sample surface in a vertical plane while the entire cavity-gear-sample assembly was immersed in a liquid-helium bath. The magnetic field direction was rotated in a horizontal plane about an axis parallel to the direction of polarization of the microwave electric field. Thus, $\mathbf{E}_{mw} \perp \mathbf{H}$ for all directions of rotation of $\mathbf{H}$. Angular increments of rotation of the sample and of magnetic field direction could be determined to within ±0.1°. This configuration allowed the study of cyclotron resonance for any angle of $\mathbf{H}$ with respect to crystallographic direction or the sample surface plane.

The entire cavity-gear assembly was constructed from nonmagnetic and nonsuperconducting materials. It was designed as a unit so that it could be hermetically sealed after mounting the sample. Because of the rapid rate of oxidation of thallium upon exposure to air, the mounting of the polished samples was performed in an inert-atmosphere dry box. After sample mounting, the cavity unit was sealed, entrapping the dry-box atmosphere inside the unit, and thus preventing surface oxidation before the assembly could be immersed in the liquid-helium bath. This procedure eliminated the need for surface coatings that might, upon freezing, strain the sample surface. Neoprene O-ring hermetic seals were used, allowing free entry of superfluid liquid helium into the cavity. All measurements were made at 1.4°K.

Variations in the real part of the sample surface impedance R were detected by measuring the real part of the cavity reflection coefficient. A homodyne reflection spectrometer and standard ac techniques were used to obtain the field derivative dR/dH, which was plotted on an x-y recorder versus the inverse magnetic field $1/H$. The magnetic field was swept as a function of time in such a manner that the dR/dH peaks of a given mass series appeared periodically in time. Shifts in peak position due to instrument time constants were then the same for each peak of a given series, and their spacing in

[26] Purchased from Union Carbide, AUC grade.
[27] Distributed by the Hirschmann Corp., 123 Powerhouse Rd., Roslyn Heights, N. Y.
[28] H. D. Guberman, J. Appl. Phys. 39, 2975 (1968).

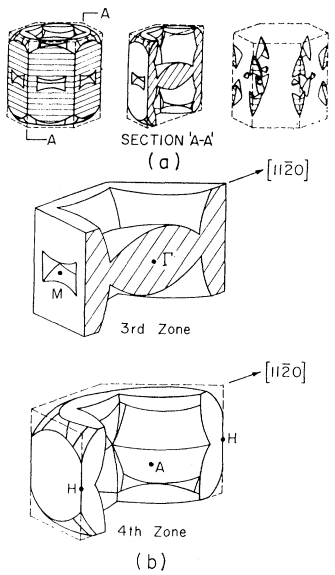

FIG. 2. NFE Fermi surface for thallium in (a) for the double-zone scheme and (b) the single-zone scheme.

$1/H$ unaffected by the magnetic field sweep rate. The magnetic field strength was measured with a Rawson rotating-coil gauss meter, which was used to calibrate each recorder plot. The resonant field value of the paramagnetic resonance of diphenyl picryl hydrazyl (DPPH) was used as a calibration check point and as the field value of the fundamental of a $m^*=m_0$ carrier. The microwave frequency was determined to within ± 0.02 GHz by using a resonant-cavity wave meter.

IV. FERMI SURFACE OF THALLIUM

Thallium has received considerable attention recently because it lends itself to a systematic study of the transition region of magnetic breakdown effects. Below 503° K[25] thallium is hcp and is known to have large sections of its FS intersecting the AHL plane of the Brillouin zone shown in Fig. 1. Falicov and Cohen[29] have shown that for hcp metals the spin-orbit interaction removes the degeneracy across the AHL plane except for the AL line, resulting in an interband energy gap that varies from some maximum at the point H to zero along the AL line. The possibility then exists for varying the position of the intercept of a carrier orbit with the AHL plane by changing the magnetic field direction and thus experimentally changing the relevant energy gap. The magnitude of the maximum energy gap in thallium has been estimated to be 0.1 eV,[6] giving rise to characteristic breakdown fields ranging from zero to more than 200 kG.[10]

The NFE model of Harrison is shown in Fig. 2(a) for the double-zone and in Fig. 2(b) for the single-zone scheme. Soven's ROPW model is shown in Figs. 3 and 4.

[29] L. M. Falicov and M. H. Cohen, Phys. Rev. **130**, 92 (1963).

Both models give a FS consisting of sheets scattered throughout the third, fourth, fifth, and sixth zones. Both models predict two sheets in the third zone enclosing unoccupied regions of k space. The large "crown" hole surface of the NFE model, centered about the point A, corresponds to the "cookie" of the ROPW model. In addition, there are small hole surfaces in the third zone centered about the point M. These pockets are shown in Fig. 2(b) for the NFE model, but are not shown in the illustrations of Soven's ROPW model. The fourth-zone surface encloses occupied regions of k space and forms a hexagonal network of connected, cylinder-like arms directed along the LHL lines. In addition, there exist 12 posts attached to the top and bottom of this network at regions near the corners of the zone. Various cross sections of these posts for the Soven model are shown in Fig. 4(b) for cuts parallel to the AHL plane. These posts have their axes directed roughly parallel to [0001]. Both models predict pockets of electrons in the fifth and sixth zones. Pockets in both of these zones are centered about the point H in both models, and are shown in Fig. 4(c) for the Soven model, while the NFE model predicts, in addition, very small pockets in the fifth zone.

In general, comparisons of the cyclotron mass anisotropy with that predicted by theoretical models is purely qualitative because of the difficulty in obtaining quantitative angular dependences from numerical band-structure calculations. However, for the NFE band structure,

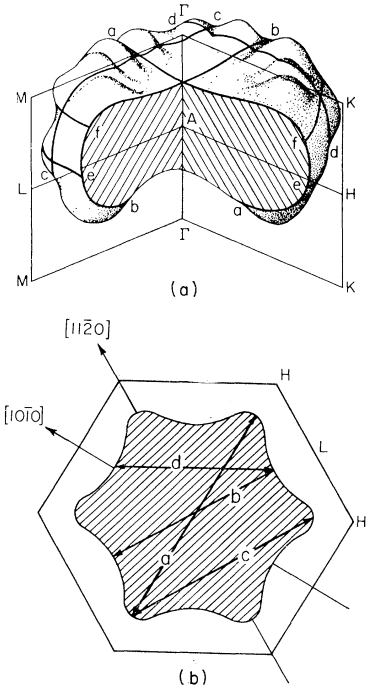

FIG. 3. Fermi surface according to Soven, enclosing unoccupied regions of k space in the third zone, is shown in (a) with possible cyclotron orbits. An AHL plane section of this surface is shown in (b) with possible orbits corresponding to those in (a).

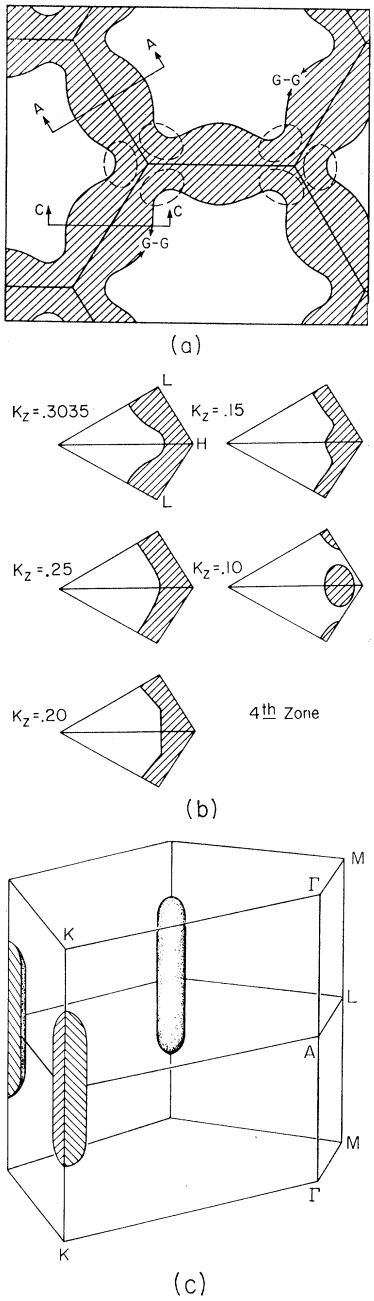

FIG. 4. Fermi surface according to Soven, enclosing occupied regions of k space in the fourth zone, is shown in (a) with possible cyclotron orbits. The section in (a) is the AHL plane, while the ovals represent sections of posts by a plane parallel to and above the AHL plane. Successive sections of the fourth-zone surface by (0001) planes are shown in (b), where the k_z values are measured from Γ along the ΓA line. The Fermi surface for the fifth and sixth zones, enclosing occupied states, is shown in (c).

one may show that the ratio of the cyclotron mass of an orbit to the mass of the free electron m^*/m_0 is given by the sum of the angles through which a carrier moves between Bragg reflections, divided by 2π.[1] It is then straightforward to calculate, using a computer, the anisotropy of the m^*/m_0 values predicted by the NFE model. This has been done for rotations of the magnetic field in the $(10\bar{1}0)$ and (0001) surfaces, using values for the lattice constants of $a=3.438$ Å and $c=5.478$ Å as measured by Barrett[30] at 5°K. Plots for some of the central orbits of the NFE model are given in Figs. 5 and 6(a).

V. RESULTS AND DISCUSSION

A. In-Plane Cyclotron Resonance

Cyclotron resonance was observed for surfaces parallel to the three major crystallographic planes, (0001), $(10\bar{1}0)$, and $(11\bar{2}0)$. The resultant curves of m^*/m_0 versus magnetic field directions in these planes are shown in Fig. 6(a) for the lower mass values and Fig. 6(b) for the higher mass values. Values of m^*/m_0 were determined by a least-squares fit to a straight line of the $1/H$ values of the dR/dH peaks versus integers. Phase shifts were negligible in all cases. Solid lines have been drawn through those mass branches where signal-to-noise ratios allowed a reasonably unambiguous determination of the periodicity of a subharmonic series. Those mass branches reported by DG[11] that were also observed in the present work are labeled in accordance with their nomenclature for ease of comparison.

At regular angular intervals the magnetic field direction was tipped out of the plane of the sample surface. The phase dependence of the various subharmonic series was studied. This information was used in main-

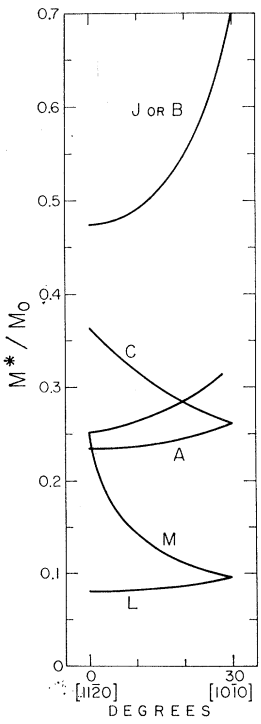

FIG. 5. Theoretical predictions of the anisotropy of some of the cyclotron masses of thallium according to the NFE model for rotations in the (0001) plane. Mass branches are labeled in agreement with their experimentally observed counterparts.

[30] C. S. Barrett, Phys. Rev. **110**, 1071 (1958).

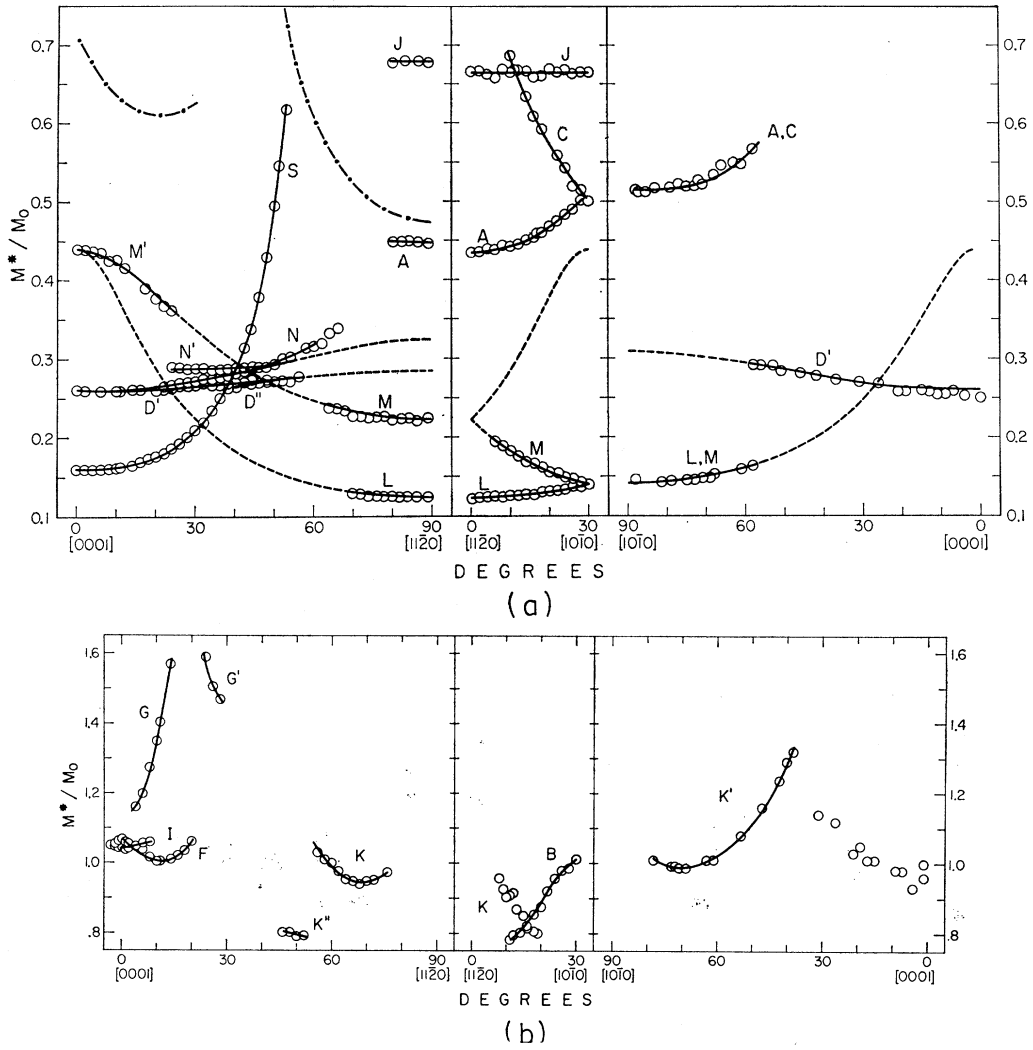

FIG. 6. Cyclotron masses in Tl as a function of the rotation of the magnetic field direction in three crystallographic planes. The dot-dash line is the predicted cyclotron mass dependence according to the NFE model for a central orbit around the third-zone hole surface. The dashed lines are fits to ellipsoidal sections of Fermi surface discussed in the text. Plot (a) covers the range $m^*/m_0<0.7$, while plot (b) covers the range $m^*/m_0>0.7$. Approximate absolute errors are given by the circle diameters.

taining the sample surfaces parallel to the static magnetic field in order to minimize errors in the determination of m^*/m_0. In addition, the information derived from the tip dependences of the signal strengths was used as an aid in assigning the various subharmonic series to orbits on the FS.

The mass branches labeled A and C, Fig. 6(a), have been assigned by DG to the arms of the fourth-zone hexagonal network. As was shown by them, the secant angular dependence is that expected for orbits enclosing cylindrical sections of FS, with the axes of the cylinders being colinear with the HLH lines. The amplitudes of the resonances giving rise to these branches are very large for magnetic field rotations in the (0001) sample surface, 35 subharmonics being observed before reaching the superconducting critical field. However, for the (10$\bar{1}$0) sample surface the resonance amplitudes were much weaker. These observations give added information concerning the shape of these arms. Figure 7 shows the real-space NFE trajectories of central orbits enclosing these arms as well as central orbits enclosing the third-zone NFE crown for $\mathbf{H}\|[11\bar{2}0]$. It is seen that the arm trajectories encounter the skin depth in the (0001) sample at points corresponding to the intersection of the k-space orbits with the AHL plane, while they encounter the skin depth of a (10$\bar{1}$0) surface at points corresponding to the intersection of the k-space orbits with the $HKLM$ plane.[31] The observed behavior leads to the conclusion that the radius of curvature of the arm

[31] These arguments, based on the well-known geometric relationship between the k-space and real-space orbits, are in direct disagreement with similar arguments proposed by DG (Ref. 11, p. 950). Spong and Kip (Ref. 16) were the first to point out the importance of these effects in observing orbits in cyclotron resonance.

orbits is small near the $HKLM$ plane and large near the AHL plane. The time of interaction of the carrier with the microwave field in the skin depth is thus larger for the (0001) surface than it is for the $(10\bar{1}0)$ sample surface, in agreement with the predicted shape of these arms.[5]

As the magnetic field direction approaches $[11\bar{2}0]$, one would expect the amplitude of the A resonances to diminish rapidly, since for this direction the central orbits about the fourth-zone arms encounter the AL line, where the spin-orbit gap is zero. Electrons on these orbits suffer complete magnetic breakdown, coupling with orbits on the third-zone hole surface to form open orbits parallel to the basal plane. These open orbits have been observed in ultrasonic attenuation[7,8] and magnetoresistance.[3,4,9,10] The large amplitude of the A-branch resonances observed for $\mathbf{H}\|[11\bar{2}0]$ in the (0001) sample suggests that the orbits contributing to these resonances originate from noncentral sections of FS considerably removed from the AL line. This is consistent with the result that the cyclotron mass need not be extremal but only slowly varying for a sufficient number of electrons of the same cyclotron frequency to contribute to an observable subharmonic series.

The branches N, N', D', and D'', Fig. 6(a), appear to be interrelated in some manner that is unclear. Nevertheless, the angular dependence of the branches N and D' for the field rotations in the $(10\bar{1}0)$ plane is seen to follow that expected from ellipsoidal surfaces (dashed lines) for either of the configurations shown in Fig. 8. The mass dependence expected from the two configurations (a) and (b) is sufficiently similar as to preclude distinguishing between them, since neither of these branches were observed for rotations of the magnetic field in the (0001) sample surface, and the scatter in the data for the $(11\bar{2}0)$ sample is too large to be conclusive. The ellipsoid parameters[32] that best fit the data are $\alpha_1=4.53$, $\alpha_2=3.27$, and $\alpha_3=2.90$, with the longest axis directed parallel to [0001]. DG also reported the branches D' and N but suggest that they are unrelated. Several observations, in addition to those presented above, support our conclusion as will be discussed in part B of this section. The resonances of both of these branches were observed for tip angles of more than 20°, indicative of small $\langle v_H \rangle$ and thus of sections with $\partial S/\partial k_H \approx 0$. Both Rayne[2] and Coon *et al.*[8] report resonances that could be assigned to these same small sections. Assuming the validity of the above conclusion concerning the relationship between the N and D' branches, it is difficult to find sections of Soven's FS that can satisfactorily account for this behavior. Soven's fifth- and sixth-zone electron surfaces are centered around the points H. As the result of the symmetry about this point one would not expect the proposed splitting for N and D'. Alternatively, one would expect this splitting for orbits enclosing the posts of the fourth-zone electron surface; however, the angular dependence and range of observability are inconsistent with this assignment. The N-branch masses are seen to deviate from the ellipsoidal fit at approximately 55° for rotations in the $(10\bar{1}0)$ sample. This is the same angular region where the branch N' is seen to merge with N and the branch D'' with D'. Beyond 55° the NN'-branch resonances were observed to be extremely narrow and quite strong until their abrupt disappearance at 64°.

Perhaps the most puzzling series observed was that giving rise to the mass branch S, Fig. 6(a). The angular dependence appears to be that expected from the minimum of an hour-glass-shaped section of FS. The tip dependence suggests that the contributing orbits may arise from sections with $\partial S/\partial k_H \approx 0$. The fundamental was observed to tip angles of 3° or 4°. The resonances of S were quite strong for rotations of $\mathbf{H}$ in the $(10\bar{1}0)$ plane, diminishing in strength for rotations beyond 40° from (0001), but nonetheless remaining quite narrow

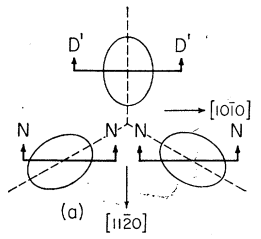

FIG. 8. Section by the AHL plane of proposed electron surfaces in the sixth zone, giving rise to the branches D' and N shown in Fig. 6(a).

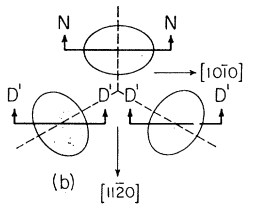

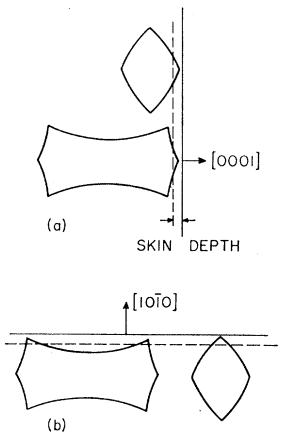

FIG. 7. The real-space trajectories of the central orbits (six-sided) around the third-zone hole surface and the arms (four-sided) of the fourth-zone electron surface for $\mathbf{H}\|[11\bar{2}0]$. Interaction of the carriers with the skin depth in a (0001) surface is shown in (a) and a $(10\bar{1}0)$ surface in (b).

[32] These parameters are defined by the equation of an ellipsoidal constant-energy surface in k space given by the expression $2m_0E/\hbar^2=\alpha_1k_x^2+\alpha_2k_y^2+\alpha_3k_z^2$. The cyclotron mass dependence for this surface may be derived using Eq. (2). See, for example, W. Shockley, Phys. Rev. **90**, 491 (1953).

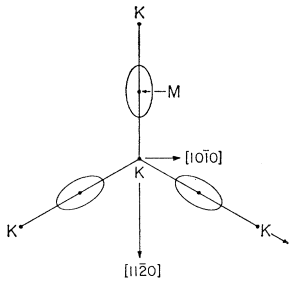

FIG. 9. Section by the ΓKM plane of the proposed small, third-zone hole surfaces that give rise to the branches L and M of Fig. 6(a).

until their disappearance at 55°. The lack of evidence for this branch with **H** in the (11$\bar{2}$0) sample surface is not surprising, since the quality of this sample was inferior to that of the (10$\bar{1}$0), as has been discussed in Sec. III. Evidence of this branch was observed in two different (10$\bar{1}$0) samples, with considerably diminished signal strengths in the inferior sample. This suggests that these orbits are particularly susceptible to surface damage and general sample quality, which may account for the lack of observation of this resonance by DG. The most reasonable assignment of branch S is to orbits enclosing the fourth-zone posts, assuming that the posts make contact at the ΓKM plane. However, the open orbits parallel to [0001] that became possible if this contact is made have not been observed in recent experiments. The ultrasonic attenuation work of Rayne[2] provides the only support for the existence of these open orbits. His interpretation in terms of open orbits has been questioned by Eckstein *et al.*[7] based on their measurements. In addition, the degeneracy of the post orbits in the Soven model would be expected to lift as the magnetic field was rotated in the plane of the (10$\bar{1}$0) sample, an effect that was not observed. This suggests that there might be a single post concentric with the KHK line. However, there is no really satisfactory explanation, short of an unpredicted sheet of FS, that is consistent with the nonobservation of open orbits.

Of particular interest are the branches L, M, and M', Fig. 6(a). They have been attributed to the small, third-zone hole surfaces predicted by both models. These surfaces are centered about the points M, with the longer axis of each surface being colinear with the KMK line, as shown in Fig. 9. The angular dependence of these branches fit, with high accuracy, that expected for ellipsoids of revolution. This angular dependence is shown as dashed lines in Fig. 6(a) for rotations of the magnetic field in the three sample surfaces. The parameters[32] of the ellipsoid that best fit this data are $\alpha_1=\alpha_3=8.00$ and $\alpha_2=0.646$. They were determined from the (0001) surface-mass dependences and the assumption of an ellipsoid of revolution. The nonobservability of these branches for some angular regions is not understood; however, it is felt that the complexity of the resonance data in these regions may have obscured these series. The observed strengths of the resonances are consistent with the assumption that the branch MM' is doubly degenerate for rotations in the (10$\bar{1}$0) plane, while branch L is due to the third ellipsoid. Of particular importance are the implications of the existence of resonances due to small sections of FS. Soven suggests that if the fourth-zone posts do not make contact with the ΓKM plane then there is the possibility that pockets of electrons will exist in this plane between adjacent posts. These pockets could give rise to the same mass dependence attributed to the hole pockets in the above analysis.

The branch G, Fig. 6(b), has been assigned by DG to the central orbit G-G around the inside of the fourth-zone hexagonal network, as shown in Fig. 4(a). The angular dependence is consistent with this orbit assignment. We observe, in addition, that the G-branch resonances are unobservable for magnetic field directions approaching to within 3° of [0001], in contrast to their results (DG, Fig. 9). As pointed out by Coon *et al.*,[8] there exists the possibility of magnetic breakdown between the orbit e-e on the third-zone cookie and this orbit G-G, since they are degenerate on the AL line. For rotations of the magnetic field in the (10$\bar{1}$0) plane, carriers on the central orbit G-G always intercept the AL lines twice in completing one revolution, while for **H**$\|$[0001] they intercept the AL lines six times. One might expect that the increase in the tunneling probability for carriers on this orbit due to the reduction of the relevant interband gap as **H** approaches [0001] would be reflected in a gradual broadening of the resonance lines. This effect was not observed. The resonance linewidths and strengths are illustrated in Fig. 10 for field directions of 4° from [0001]. For field directions of 3° and less from [0001] the resonance line strengths diminished abruptly. This behavior was confirmed to be symmetric about [0001] for field rotations in the plane. Blount[33] has shown that the probability for magnetic breakdown across an interband energy gap is given by $P=e^{-H_0/H}$, where H_0 is a characteristic breakdown field dependent upon the size of the gap and upon the carrier velocity direction. Moore[34] has proposed that the relative linewidths for cyclotron resonance involving magnetic breakdown effects may be written as $\Delta H/H_n \approx (n\omega_c\tau)^{-1}+(2\pi n)^{-1}rP$, where n is the subharmonic number, r is the number of equivalent breakdown points encountered by the carrier in completing one k-space orbit, and where $P\approx 0$. It is apparent that the increase in r from 2 to 6 cannot alone account for the disappearance of branch G. However, one must take into account the velocity-direction dependence of P, as has been emphasized by Young.[10] It is then possible that the exponential dependence of P on velocity direction in the neighborhood of the breakdown point could account for this behavior. However, it is not clear that magnetic breakdown effects are solely responsible for the nonobservability of the G-branch resonances with **H**$\|$[0001], since other factors such as mass spread may be involved.

[33] E. I. Blount, Phys. Rev. **126**, 1636 (1962).
[34] T. W. Moore, Phys. Rev. Letters **18**, 310 (1967).

Indeed, for this field direction one would expect that the resonance would be strongest, since the carriers in the vicinity of the central orbit *G-G* arise from almost cylindrical sections of FS formed by the sides of the fourth-zone arms, with only a small fraction of the carriers actually intercepting the *AL* line. However, no alternative assignment for the branch *G* can be made at this time.

The branch *F*, Fig. 6(b), has been assigned by DG to what are termed "shadow" orbits on Soven's third-zone hole surface. These noncentral orbits lie above and below the *AHL* plane and are illustrated in Fig. 3(a) as *f-f*. In addition to *F*, a branch *I* was observed, which may be a splitting of the branch *F*. The amplitudes of the resonances of both branches diminish rapidly with increasing tip angle and were also seen to shift towards lower mass. This suggests that the orbits giving rise to these resonances have a considerable orbit-average velocity component along the magnetic field direction, characteristic of noncentral orbits and consistent with the DG assignment. The splittlng may be due to the misalignment of the sample surface with the $(10\bar{1}0)$ plane, although Laue photographs indicate an accuracy of $\pm 1°$. A slight misalignment could cause the selection of shadow orbits lying in planes with slightly differing values of $|k_H|$ due to differing geometries of the real-space trajectories in the region where the carrier passes through the skin depth.

An alternative assignment for the *F* and *I* branches arises from the qualitative similarity of the angular dependence of the branch *F* to the angular dependence of the central orbit of the type *e-e* of Fig. 3(a), but referred to the NFE crown. The minimum in the branch *F* occurs at approximately 11°, while the minimum predicted by the NFE model occurs at approximately 21° as shown by the dot-dash line in Fig. 6(a). This discrepancy does not seem excessive, since the introduction of a finite crystal potential would be expected to round off the cusps of the NFE model and shift the position of the minumum. In this interpretation, the branch *I* would be due to the noncentral shadow orbits. Further support for this interpretation is provided by the angular dependences and ranges of observability of both branches. However, the tip dependence discussed above is inconsistent with this interpretation, as is the lack of evidence for magnetic breakdown effects. Magnetic breakdown effects were observed by DG in their $(11\bar{2}0)$ sample for resonances that they assign to the *e-e* orbit. It is not likely that the branch *I* is due to the Doppler splitting as discussed by Koch *et al.*,[14] since the separation between the *I* and *F* resonances does not show the expected change with tip angle.

In a $(10\bar{1}0)$ sample of an inferior quality to the one giving rise to the data of Fig. 10, the *I* and *F* resonances were sinusoidal in $1/H$ and distinguishable only by the existence of beating between high-integer subharmonics. Strong beating was also characteristic of the $m^*/m_0 \approx 1$

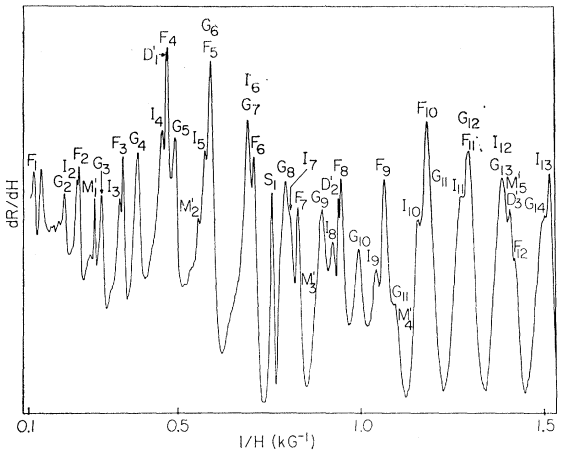

FIG. 10. Cyclotron-resonance spectra observed in thallium for **H** at an angle of 4° with [0001] in the $(10\bar{1}0)$ sample surface.

resonances observed for magnetic field directions near [0001] in the $(11\bar{2}0)$ surface. Since the $(11\bar{2}0)$ sample exhibited a rather low $\omega_{mw}\tau$, particularly for this region, the two resonances could not be resolved. However, very distinct nodes and antinodes were observed for the high-integer subharmonics. The fundamental and first few subharmonics were unobservable in our work, in agreement with the observations of DG. They attribute this behavior to magnetic breakdown effects and assign these resonances to the central orbit *e-e* around the third-zone cookie. Unfortunately, the ambiguity in the determination of the periodicity of the subharmonic series due to the above factors precludes the drawing of lines through data points for this angular region for the $m^*/m_0 \approx 1$ masses.

The branches *K* and *K'* observed in the $(10\bar{1}0)$ and $(11\bar{2}0)$ samples, respectively, have similar angular dependences, with a minimum occurring at approximately 68° from [0001] for each case. The branch *K'* has an identical angular dependence and range of observability, but has twice the value of m^*/m_0, as does the branch *B* reported by DG in this plane. Neither the branch *D* nor the branch *B* reported by DG were observed by us. This leads to the conclusion that their branch *D*, along with their branch *B*, constitute our branch *K'*. They report a phase shift of $n_0=\frac{1}{2}$ for the *D* branch, thus accounting for the odd subharmonics of the branch *K'*, while their branch *B* accounts for the even subharmonics. There was seen to be a definite correlation in the shift of all derivative peaks of this branch as the field was rotated in the plane. A similar situation holds true for the branch *D* as reported by DG for their $(10\bar{1}0)$ sample, although they report no branch *B* for this orientation. Examples of the resonances for these two samples are shown in Fig. 11, where the magnetic field directions are approximately 65° away from [0001] for both cases.

Orbits for a similar range of magnetic field directions have been reported by Coon *et al.*,[8] and by Priestley[6]

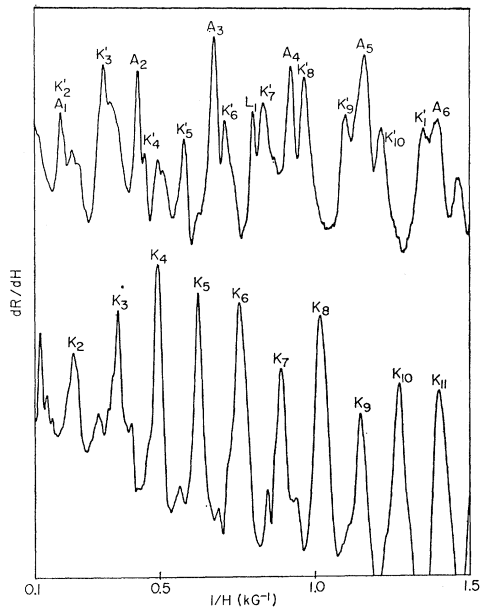

FIG. 11. Examples of the cyclotron-resonance spectra of the K and K' branches for field rotations in the $(10\bar{1}0)$ and $(11\bar{2}0)$ sample surfaces for **H** at an angle of approximately 68° with [0001].

and have been assigned by them to the noncentral orbits on the third-zone surface. In particular, the branch K in the $(10\bar{1}0)$ surface corresponds to an orbit of the type c-c, while the branch K' in the $(11\bar{2}0)$ surface corresponds to an orbit of the type d-d. The amplitudes of these resonances do not diminish rapidly with increasing tip angle, suggesting that their $\langle v_H \rangle$ is small, inconsistent with the noncentral-orbit interpretation. It is to be further noted that the range of observability of the K' branch seems to be too great for this interpretation. Notwithstanding, a similar angular range is observed by Coon *et al.*[8] in their ultrasonic studies. The branch K, as observed in the (0001) sample, has a certain similarity to the branch H reported by DG, except for a factor of 2. The branch H was observed by DG only in their $\mathbf{E}_{\mathrm{mw}} \| \mathbf{H}$ experiments so that the lack of evidence for this branch for our $\mathbf{E}_{\mathrm{mw}} \perp \mathbf{H}$ configuration is not surprising. There was some ambiguity in the mass determination and lines have not been drawn through our data points.

The branch B observed in the (0001) sample is another case where the angular dependence is identical to the branch B reported by DG, but differs by a factor of 2 in the values of m^*/m_0. An example of the data for this branch is shown in Fig. 12. There was seen to be a definite correlation in the shift of all derivative peaks of this branch as the field was rotated in the plane. Upon careful examination of the data, no evidence of the B branch of DG was found in our work. Assignment of this branch to the central orbit around the third-zone crown of the NFE model is based upon the similarity of its angular dependence to that predicted by the NFE model as shown in Fig. 5. The weak resonance amplitudes for **H** parallel to and approaching $[10\bar{1}0]$ and for **H** approaching $[11\bar{2}0]$ provides support for this assignment, since for $\mathbf{H} \| [10\bar{1}0]$, central orbits on the NFE crown are in a region of large dm^*/dk_H, while for $\mathbf{H} \| [11\bar{2}0]$ these orbits contact the AL line.

The mass branch J, Fig. 6(a), has been assigned by DG to the central orbits around the third-zone cookie such as b-b and a-a shown in Fig. 3(a). The angular dependence, to within our experimental uncertainty, is isotropic, in strong disagreement with the NFE predictions, as has been discussed above for branch B. For magnetic field directions approaching $[11\bar{2}0]$ the resonance amplitudes arising from central orbits around the cookie would be expected to decrease rapidly for the same reasons as discussed in connection with the fourth-zone arms. The large resonance amplitudes observed for the branch J with $\mathbf{H} \| [11\bar{2}0]$ suggest that if this assignment is correct, the orbits contributing to these resonances must arise from noncentral sections of FS, thus being somewhat removed from the AL line. This argument was also advanced by Soven[5] in connection with Priestley's[6] de Haas–van Alphen data. It is to be noted that if the assignments to the third-zone cookie for the branches K and K' are correct, then the above assignment for J is open to serious question. The value of $m^*/m_0 \approx 0.67$ for the branch J appears to be much too low in comparison with values of $m^*/m_0 \approx 1.0$ for K and K'. Supporting DG's assignment, the large resonance amplitudes for the (0001) sample suggest that they arise from a section with very little m^* versus k_H variation, as is characteristic of the central orbit around the Soven-model cookie. In addition, the lack of observability of J-branch resonances for the $(11\bar{2}0)$ surface and the small angular region of observability of very weak resonances in the $(10\bar{1}0)$ sample can be explained in terms of the trajectory shape as shown in Fig. 7, together with arguments similar to those presented for the fourth-zone arms. DG report evidence for the branch J in their $(11\bar{2}0)$ samples; however, our data is inconclusive on this point.

The branches G' and K'', Fig. 6(b), exist for only small angular regions of rotation of **H** in the $(10\bar{1}0)$

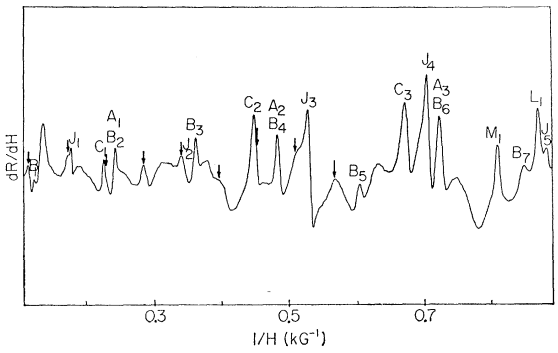

FIG. 12. Cyclotron-resonance spectra observed in thallium for **H** at an angle of 4° with $[10\bar{1}0]$ in the (0001) sample surface.

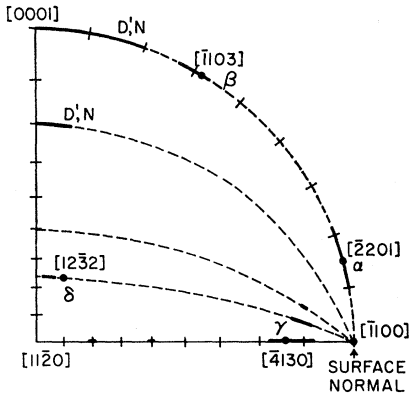

FIG. 13. Angular regions of magnetic field direction where tipped-field cyclotron resonance was observed for a $(10\bar{1}0)$ surface.

plane. G' could be assigned to central orbits around the inside of the fourth-zone network near the base of the posts if the posts lean toward the center of the zone as predicted by the NFE model. In this case, G' would be the extension of branch G, but this assignment is very tentative. No assignment has been made for the branch K''. In addition, several resonances were seen in all sample surfaces, where unambiguous period determinations were not possible or where the resonances could not be followed through a useful angular interval. An example of this (marked by arrows) is given in Fig. 12 and tentatively assigned a value of $m^*/m_0 \approx 2$. This series could be followed for only 3° or 4°, with the amplitude diminishing rapidly as the field was rotated away from $[10\bar{1}0]$.

B. Tipped-Field Cyclotron Resonance

Limited studies of small-angle tipped-field cyclotron resonance were conducted on (0001) and $(11\bar{2}0)$ sample surfaces, while more extensive preliminary studies were conducted on the $(10\bar{1}0)$ surface for tip angles of up to 90°. Some of the directions for which tip resonances were observed for the $(10\bar{1}0)$ surface are shown in the Wullf stereographic projection, Fig. 13. Figure 14 illustrates the tip dependence for the $(10\bar{1}0)$ sample of a representative subharmonic resonance of the series giving rise to the branches D' and N, Fig. 6(a). These branches were shown in part A of this section to fit the angular dependences expected of the ellipsoidal sections of FS shown in Fig. 8. The tip dependence illustrated is for **H** tipped out of the $(10\bar{1}0)$ sample surface from its in-surface direction of 20° from [0001]. This behavior was observed to be symmetric about the in-surface field direction, and except for the splitting at 19.7° and the very small splitting at 0°, it is identical to the tip dependence observed for **H** tipped from an in-surface direction parallel to [0001]. There was no inversion of derivative peaks as was observed by Koch *et al.*[14] for small-angle tipping in copper. The complete degeneracy observed for the D'- and N-branch resonances for **H**$\|$[0001] and zero tip angle and their splitting for a tip angle of 7.7° suggests that these two branches are indeed related. The further splitting at 19.7° observed for **H** tipped out of the surface in a nonsymmetry plane and the lack of evidence for this splitting for **H** tipped out of the surface in a $(11\bar{2}0)$ plane suggest further that three related orbits are contributing to the observed resonances. These orbits could arise from sections of FS such as the ellipsoids illustrated in Fig. 8.

Of special note is the strengthening of those resonances as the field is tipped out of the surface. Due to the observed symmetry of this effect about the in-surface field direction, it is felt that it is due primarily to Doppler effects. If the range of cyclotron frequencies (mass spread) is large for carriers contributing to a resonance then interference effects between the contributions of the various carriers within this range tend to diminish and broaden the resonance peaks. In our opinion, this situation corresponds to 0° of Fig. 14. As the field is tipped out of the plane of the sample surface, the Doppler broadening of these peaks, due to a finite $\langle v_H \rangle$, is more than compensated for by the narrowing

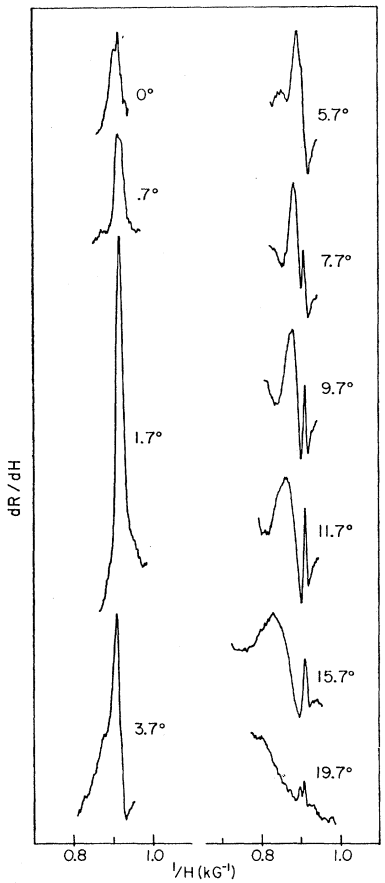

FIG. 14. Tip dependences of the line shape of representative $(n=2)$ subharmonic of the D' and N resonances. Angular designations give the angle of the magnetic field direction with the sample surface. This tip dependence was seen to be symmetric about 0°.

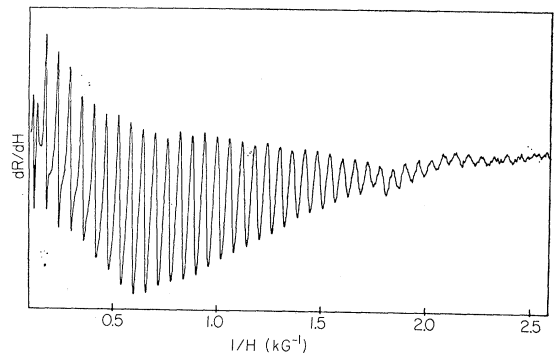

FIG. 15. Example of the α resonances of Fig. 13 for **H** at an angle of 79° with [0001].

brought about by the selection of carriers with small $\langle v_H \rangle$ that also have a small mass spread. In our opinion, this situation corresponds to the 1.7° trace. The further broadening and shifting to higher fields of the one peak may be due to the Doppler broadening of a group of carriers centered about a central orbit ($\langle v_H \rangle = 0$). The shift to higher fields is then a reflection of the anisotropy of the cyclotron mass of the central orbit, while the width of the resonances reflects the increasing component of $\langle v_H \rangle$ of noncentral orbits in this group as the tip angle is increased. The above explanation is not consistent, however, with resonances due to carriers on ellipsoidal surfaces, since for that case all carriers have the same cyclotron period and thus no mass spread. Nor is the difference in observed linewidths of the tilt resonances consistent with the ellipsoidal surfaces of Fig. 8. These ellipsoids were tentatively found to be nearly spherical, thus one would not expect the distribution of values of $\langle v_H \rangle$ that lead to Doppler broadening to vary much with the orientation of the ellipsoid with respect to the sample surface.

Of particular interest are the large-amplitude resonances observed for the various angular regions designated by Greek letters in Fig. 13. In most cases, these resonances were as strong as the in-surface resonances. An example of the α resonances is shown in Fig. 15 for a tip angle of 79° from (0001) in the $(10\bar{1}0)$ sample surface and for **H** in the $(11\bar{2}0)$ plane. In general, these resonances are characterized by very large anisotropy in both mass and amplitude, sinusiodal line shapes and very small phase shifts. In some cases, a 30% change in values of m^*/m_0 within a 5° interval were observed. Several workers[15,35–37] have observed large-amplitude tip resonances for field directions up to 90° from the sample surface. The resonances observed in thallium are very similar to the recent observations of Khaikin and Cheremisin[38] (KC) in their tipped-field experiments on tin. KC attribute this behavior to large extended orbits, enclosing several cells in reciprocal space, and suggest that the carriers may enter the skin depth at several places in the orbit during a k-space revolution. Resonance may occur whenever the period of motion of the carrier between its successive entries into the skin depth is equal to nT_{mw}, where n is an integer. The relative linewidth $\Delta H/H$ is determined by the number of skin depth encounters m and is proportional to m^{-1}. The narrowest lines would occur when the cyclotron period and the period of successive encounters are both multiples of T_{mw}, a situation that produces the largest number of in-phase skin depth encounters before scattering. The least number and hence the broadest linewidths occur when the carrier makes only two or three encounters before disappearing into the bulk of the metal or returns out of phase with the microwave electric field. This explanation for the observed behavior in tin seems to account for the observed behavior in thallium. For the α, β, and γ regions, the resonances became broad and very weak for field directions near a minimum in the m^*/m_0 versus tip-angle dependence. These directions occur to within $\pm 2°$ of the crystallographic directions shown in Fig. 13 within the ranges of observability. In agreement with KC, it is felt that for these directions, the carrier encounters the skin depth in phase with $\mathbf{E}_{\mathrm{mw}}$ only a few times and upon completion of a k-space orbit returns out of phase. These resonances were also observed to disappear very abruptly at the extrema of these ranges, sometimes within a tip interval of one-tenth of a degree.

It is important to point out the possibility of extended orbits due to magnetic breakdown through regions near the AL line. This would correspond to $P \approx 1$. Moore[34] points out that for this case, the relative linewidths of the cyclotron-resonance peaks may be written as $\Delta H/H_n \approx (n\omega_c\tau)^{-1} + (2\pi n H_n)^{-1} r H_0$. Thus, broadening due to magnetic breakdown effects is indistinguishable from ordinary scattering, since both mechanisms exhibit the same field dependence. An example of this might be the α resonances shown in Fig. 15. These resonances occur in a region of magnetic field direction corresponding to that of the mass branch K' seen in the $(11\bar{2}0)$ surface, and have values of m^*/m_0 that are roughly twice those of this branch. These observations suggest that the α resonances may be due to extended orbits in the vicinity of the noncentral orbits d-d shown in Fig. 3, in which case two sets of carriers would be expected for orbit planes passing through those regions of small breakdown field near the AL lines.

The δ resonances appeared within a 3° tip in the region of in-surface field direction where the resonances of the K branch were observed. The m^*/m_0 values are very nearly double that of the K branch; however, the K branch resonances did not exhibit any of the mass doubling or peak inversion characteristics of the Doppler-shifted resonances as observed by Koch *et al.*[15] in copper, or the current-sheet resonances observed by

[35] D. G. Howard, Phys. Rev. **140**, 1705 (1965).
[36] D. N. Langenberg and S. M. Marcus, Phys. Rev. **136**, A1383 (1964).
[37] J. F. Koch and A. F. Kip, Phys. Rev. Letters **8**, 473 (1962).
[38] M. S. Khaikin and S. M. Cheremisin, Zh. Eksperim. i Teor. Fiz. **54**, 69 (1968) [English transl.: Soviet Phys.—JETP **27**, 38 (1968)].

Spong *et al.*[16] in aluminum. The resonances apparently are due to two different sets of carriers, since a very strong beating was observed, as was true for some regions of observability of α and γ resonances.

The γ resonances ($0.9 \lesssim m^*/m_0 \lesssim 1.2$) were observed for tipping in the basal plane as well as for tipping in other planes as shown in Fig. 13. The range of observability is seen to diminish as the plane of tip is rotated away from the basal plane; however, the m^*/m_0 values change little. For field-tip directions of $\pm 10°$ from [1010] in the basal plane, resonances are observed that have the same value of m^*/m_0 as for the tip direction of 10° from [1100] but greatly diminished in strength. These resonances may be due to almost stationary noncentral orbits on the third-zone hole surface of the type *c-c*, thus accounting for the existence of two resonances in the same region of field. Ratios of amplitudes of these two resonances varied considerably in the range of observability.

Characteristic of all of these large tip-angle resonances was the sharp derivative maximum for the low-integer subharmonics, suggesting that they are due to surface-impedance minima and not the surface-impedance maxima that would arise from the anomolous penetration of microwave field into the depth of the sample as proposed by Kaner and Blank[39] for tipped-field cyclotron resonance. These observations for thallium are in agreement with the observations of KC for tin.

C. Mass Enhancement Factor

Comparisons of the predictions of the NFE model with the experimental results give values of the mass enhancement factor m^*/m^*_{NFE}, ranging from 1.4 for masses attributed to the third-zone electron surface to 1.8 for masses of the fourth zone. As pointed out by Harrison,[40] these discrepancies cannot be accounted for by the introduction of a finite pseudopotential. Nakajime and Watabe[41] have shown that this discrepancy is due to many-body interactions, which affect the thermal mass (specific heat) and the cyclotron mass in the same fashion. Ashcroft and Wilkins[42] have calculated the electronic contribution to the low-temperature specific heat for three nontransition metals. They have shown that the electron-phonon interaction accounts for most of the discrepancy between measured thermal masses and those calculated from single-particle band structures. Their calculated thermal mass enhancement factors agree closely with experimental values for sodium, aluminum, and lead. They point out that there is also good agreement between the experimental values of the thermal and cyclotron mass enhancement factors for these metals. Table I lists the results of the electronic specific-heat measurements in thallium along with values of the thermal mass enhancement factor m^*_{SH}/m_0. It is seen that the results of Snyder and Nicol[43] fall within the range of cyclotron mass enhancement factors observed in this work, while the results of Maxwell and Lutes[44] and van der Hoeven and Keesom[45] are much smaller. The values given by van der Hoeven and Keesom would appear to be the most reliable due to the range of temperatures involved in their measurement, thus allowing them to more reliably separate electronic and lattice contributions. No explanation for these discrepancies can be offered at this time.

TABLE I. Summary of electronic specific-heat measurements on thallium, including the thermal mass enhancement factor m^*_{SH}/m_0.

	Temperature range (°K)	γ (mJ/mole deg^2)	M^*_{SH}/M_0
Snyder and Nicol[a]	1.1–4.2	2.56	1.73
Maxwell and Lutes[b]	1.2–4.2	1.53	1.18
van der Hoeven and Keesom[c]	0.4–4.2	1.47	1.14

[a] Reference 43. [b] Reference 44. [c] Reference 45.

VI. SUMMARY

Measurements of the cyclotron masses of thallium have been made for rotations of the magnetic field in (0001), (10$\bar{1}$0), and (11$\bar{2}$0) sample surfaces. Results were not conclusive as to the validity of the ROPW model of Soven over the NFE model; in fact, cyclotron orbits were observed that cannot be accounted for by either model. Observed cyclotron mass enhancement factors were found to disagree with the most recent measurements of the thermal mass enhancement factors.

Certain mass branches were observed with values of m^*/m_0 exceeding by a factor of 2 those of similar anisotropies and ranges of observability reported by DG. It is felt that the higher resolution due to superior signal-to-noise ratios of the measurements reported in this work may account for this discrepancy. Bulk damage caused by spark-erosion cutting was observed and is felt to be responsible for the poorer signal-to-noise ratios observed for the (11$\bar{2}$0) samples used in this work, and may account for the lack of observation of certain orbits in previous FS measurements made by other workers.

Tipped-field resonances were observed for the (10$\bar{1}$0) sample surface which were accounted for, in a qualitative fashion, by the extended orbit mechanism proposed by Khiakin and Cheremisin; however, definite orbit assignments for these resonances were not possible.

[39] E. A. Kaner and A. Y. Blank, J. Phys. Chem. Solids **28**, 1735 (1967).
[40] W. A. Harrison, *Pseudopotentials in the Theory of Metals* (W. A. Benjamin, Inc., New York, 1966).
[41] S. Nakajima and M. Watabe, Progr. Theoret. Phys. (Kyoto) **30**, 772 (1963).
[42] N. W. Ashcroft and J. W. Wilkins, Phys. Letters **14**, 285 (1965).
[43] J. L. Snyder and J. Nicol, Phys. Rev. **105**, 1242 (1957).
[44] E. Maxwell and O. S. Lutes, Phys. Rev. **95**, 333 (1954).
[45] J. C. van der Hoeven, Jr., and P. H. Keesom, Phys. Rev. **135**, A631 (1964).